Rao, Bin; Hu, Jie; Al-nahari, Azzam; Yang, Kun; Jantti, Riku

On the Physical Layer Security of UAV-Aided Backscatter Communications

Published in:
IEEE WIRELESS COMMUNICATIONS LETTERS

DOI:
10.1109/LWC.2023.3324914

E-pub ahead of print: 01/01/2023

Document Version
Peer-reviewed accepted author manuscript, also known as Final accepted manuscript or Post-print

Please cite the original version:
Rao, B., Hu, J., Al-nahari, A., Yang, K., & Jantti, R. (2023). On the Physical Layer Security of UAV-Aided Backscatter Communications. *IEEE WIRELESS COMMUNICATIONS LETTERS*. Advance online publication. https://doi.org/10.1109/LWC.2023.3324914

On the Physical Layer Security of UAV-aided Backscatter Communications

Bin Rao, Jie Hu, *Senior Member, IEEE*, Azzam Al-nahari, Kun Yang, *Fellow, IEEE*, Riku Jäntti, *Senior Member, IEEE*

***Abstract*—In this letter, we investigate the issue of physical layer security in unmanned aerial vehicle (UAV)-assisted backscatter communication. The scenario involves a single UAV, a single passive backscatter device (BD), in the presence of a single eavesdropper (ED) attempting to intercept the backscattered information from the BD. To counteract the ED's efforts, we propose an artificial noise (AN) injection scheme to degrade the ED link. We aim to maximize the secrecy rate of the BD by optimizing three key factors: the UAV's hovering position, the power allocation factor, and the reflection coefficient of the BD. For this system setting, we derive the secrecy rate and formulate an optimization problem to optimize these variables. Due to the non-convex nature of the problem, we design an iterative algorithm based on the alternating optimization (AO) algorithm for maximizing the secrecy rate. Additionally, we provide insights into the impact of various system parameters on the overall performance. Notably, we demonstrate that the power allocation factor and the hovering altitude of the UAV play important roles for achieving secure communication.**

***Index Terms*—Unmanned aerial vehicle (UAV), backscatter communications, physical layer security, artificial noise (AN).**

I. Introduction

The rapid and massive deployment of Internet of things (IoT) devices has the potential to transform industries, enhance efficiency, and improve quality of life. However, one of the key challenges is that IoT devices are often deployed in remote or hard-to-reach locations, making battery replacement or recharging difficult. Backscatter communication is a promising technique that enables IoT devices to extend their lifetime by conserving energy and reducing power consumption [1]. Unfortunately, due to the variability of the ambient signal and the power constraint of the backscatter device (BD), the transmission range of the BD is limited, which impose challenges for data collection. Unmanned aerial vehicles (UAVs) is an emerging technology with many applications including data collection in wireless sensor networks [2]. The integration of UAV with backscatter communication presents a promising and cost-effective solution for upcoming IoT services. [3], [4].

Furthermore, securing backscatter communication is crucial for data protection due to size, cost, and computation constraints. Physical layer security is a promising means to ensure secrecy [5]. Numerous techniques to secure backscatter communication systems can be found in the existing literature [5]–[9]. In [5], an artificial noise (AN) injection scheme was proposed to secure monostatic backscatter systems. Optimal tag selection schemes were proposed in [6] to enhance transmission security. The work in [7] investigated AN- assisted MIMO system to safeguard the radio frequency identification (RFID) systems. In [8], an AN injection scheme to improve the secrecy capacity of the backscatter channel in a multi-BD wireless powered backscatter communication was proposed. The work in [9] proposed an AN-assisted beamforming for enhancing secure transmission in symbiotic radio systems. On the other hand, securing UAV communications raises additional challenges due to the line-of-sight (LoS) links of the air-to-ground (A2G) and ground-to-air (G2A) links [10]. In [11], the authors maximized the uplink fair secrecy rate of backscatter sensor nodes by jointly optimizing the backscattering coefficients, the scheduling, and the UAV trajectory. In [12], analog beamforming and randomized continuous wave were proposed for securing multiple BDs and the secrecy rate is maximized by jointly optimizing the beamforming, the UAV's location and random continuous wave setting.

In this letter, we address the issue of physical layer security in UAV-assisted backscatter communication systems. Specifically, we propose the use of AN technique to enhance the security of these systems. Our objective is to optimize the power allocation factor, reflection coefficient, and hovering position of the UAV to maximize the secrecy rate. While the concept of AN has been utilized in previous studies on physical layer security, specifically in traditional cellular systems as mentioned in [13] and [14], and in the context of backscatter communications as discussed in [5] and [9], its application to UAV-assisted backscatter communications is novel. This letter presents the following key contributions.

1) We propose an AN injection scheme for secure transmissions in UAV-assisted backscatter communications.
2) We present the formulation and solution of an optimization problem aimed at maximizing the secrecy rate. This is achieved by jointly optimizing the power allocation factor, the reflection coefficient, and the hovering position of the UAV. We design an iterative algorithm based

This work was supported in part by the Natural Science Foundation of China under Grant 61971102, in part by the Sichuan Science and Technology Program under Grant 2022YFH0022, in part by the Stable Supporting Fund of national Key Laboratory of Underwater Acoustic Technology, in part by the Key Research and Development Program of Zhejiang Province (No. 2022C01093).

The work of Riku Jäntti and Azzam Al-nahari was supported in part by the European Project Hexa-X II, and in part by the Business Finland Project 6G-eMTC. The views and opinions expressed are however those of the authors only and do not necessarily reflect the views of Hexa-X-II Consortium.

Bin Rao, Jie Hu and Kun Yang are all with the Yangtze Delta Region Institute (Huzhou) and School of Information and Communication Engineering, University of Electronic Science and Technology of China, Huzhou, 313001, China, email: 202122010628@std.uestc.edu.cn, hujie@uestc.edu.cn, kunyang@essex.ac.uk, (*Corresponding Author: Jie Hu.*)

Azzam Al-nahari is with the Department of Information and Communications Engineering, Aalto University, Espoo, Finland, and also with the Department of Electrical Engineering, Ibb University, Ibb, Yemen (e-mail: azzamyn@gmail.com).

Riku Jäntti is with the Department of Information and Communications Engineering, Aalto University, Espoo, Finland, (e-mail: riku.jantti@aalto.fi).

This article has been accepted for publication in IEEE Wireless Communications Letters. This is the author's version which has not been fully edited and content may change prior to final publication. Citation information: DOI 10.1109/LWC.2023.3324914

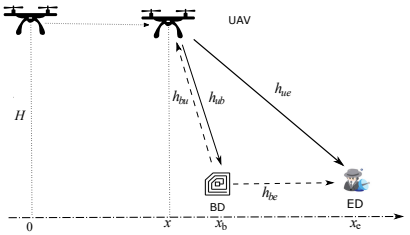

Fig. 1. Illustration of a secure communication model of UAV-assisted backscatter communication system, in the presence of an eavesdropper (ED).

on the alternating optimization (AO) algorithm, which allows us to iteratively and efficiently solve the problem.

3) We deliver comprehensive numerical results to substantiate the efficiency of our suggested optimization strategies, and to assess the impact of various system parameters on the secrecy performance.

II. System and Channel Models

We consider a secure communication scenario in the context of UAV-assisted backscatter communications as shown in Fig. 1, which consists of a UAV, a backscatter device (BD), and an eavesdropper (ED) that is trying to overhear and intercept the transmission from the BD. We assume that all nodes are equipped with a single antenna. To facilitate the analysis, we utilize a two-dimensional Cartesian coordinate system to denote the position of each entity. Specifically, the BD and ED are situated on the ground, and their respective coordinates are fixed as $(x_b, 0)$ and $(x_e, 0)$. The UAV starting point is $(0, H)$. The UAV is assumed to fly at fixed altitude H and fixed speed, so that its coordinate (x, H) is variable according to the horizontal coordinate x. For the information transmission from the BD, we employ a backscatter communication mechanism where the UAV assumes the role of the reader in a monostatic backscatter communication [15]. Specifically, the UAV first transmits a single carrier signal s to power up the BD, where $\mathbb{E}[|s|^2] = 1$, and a noise-like $z \sim \mathcal{CN}(0, 1)$ to degrade the ED link. Thus, the total transmitted signal by the UAV is given as

$$x = ps + qz, \tag{1}$$

where p and q represent the power of the carrier and noise signals, respectively. The total transmit power budget at the UAV is denoted as P_c, while $0 < \phi \leq 1$ represents the fraction of power allocated to the information signal. Hence, we have

$$p = \phi P_c \quad \text{and} \quad q = (1 - \phi) P_c \tag{2}$$

Next, the BD incorporates the information data onto the carrier signal and reflects it back to the UAV. During the data collection process, the UAV hovers above the BD at the horizontal distance x until the data transmission is completed.

As shown in Fig. 1, the distance between the UAV at any point and the BD is $d_{ub} = \sqrt{H^2 + (x_b - x)^2}$. Similarly, the distance between the UAV and ED is $d_{ue} = \sqrt{H^2 + (x_e - x)^2}$, and the distance between the BD and the ED is $d_{be} = (x_e - x_b)$ The channels of UAV-BD, BD-UAV, UAV-ED, and BD-ED are denoted as h_{ub}, h_{bu}, h_{ue}, and h_{be}, respectively. Since single-antenna nodes is assumed, the forward channel h_{ub} and and the reverse channel h_{bu} can be assumed to be equal. Due to the strong LoS propagation of the A2G channels, we consider a pure distance-based model for h_{ub} and h_{ue}. Furtehrmore, from the worst-case perspective, we assume that the ED is in close proximity to BD, which implies that h_{be} can be modeled as LoS channel [16]. Therefore, the different channels are given as follows

$$h_a = \sqrt{\frac{\Omega}{d_a^{\varpi}}} \tag{3}$$

where $a \in \{ub, ue, be\}$, Ω represents the average channel attenuation at unit reference distance, i. e., $\Omega = (\frac{3\times10^8}{4\pi f})^2$, and ϖ is the path loss exponent. Now, neglecting the reflection noise at the BD, the received signal at the UAV is given as

$$y_u = \sqrt{\alpha p} h_{ub}^2 sb + \sqrt{\alpha q} h_{ub}^2 zb + n_u, \tag{4}$$

where the first term is the useful signal, and b is the information signal reflected by the BD, where $\mathbb{E}[|b|^2] = 1$. The last two terms represent the combined noise. We assume that both s and b are circularly symmetric Gaussian each with zero mean and unit variance, α is the reflection coefficient of the BD, and $n_u \sim \mathcal{CN}(0, \sigma_u^2)$ is the AWGN. It should be noted that despite the UAV having prior knowledge of the transmitted AN signal, recovering the backscattered value becomes challenging without proper channel training and tracking. This difficulty arises from the AN round-trip path and its associated unknown time and phase shift [5], [8]. To address the potential scenario of the UAV partially canceling the backscattered AN signal, we will introduce an attenuation factor denoted as $0 \leq \kappa \leq 1$, which quantifies the UAV's success in canceling the backscattered noise. $\kappa = 0$ means that the UAV is able to filter out all the transmitted AN signal, and $\kappa = 1$ means that all the AN signal is also considered at the UAV receiver. The SNR at the UAV is thus given by

$$\gamma_u = \frac{\alpha p \Omega^2 d_{ub}^{-4}}{\kappa \alpha q \Omega^2 d_{ub}^{-4} + \sigma_u^2} \tag{5}$$

Similarly, the received signal at the ED is given as

$$y_e = \sqrt{\alpha p} h_{be} h_{ub} sb + \sqrt{\alpha q} h_{be} h_{ub} zb + \sqrt{q} h_{ue} z + n_e \tag{6}$$

where the first and second terms represent the bckscattered signal and noise from the BD, respectively. The third term represent the AN received directly from the UAV. $n_e \sim \mathcal{CN}(0, \sigma_e^2)$ is the AWGN. We assume that, in normal backscatter systems, the standardized carrier wave signal is known to the ED, and hence, can be easily removed from the received signal. This is why the signal term $\sqrt{p} h_{ue} s$ does not appear in (6). Therefore, the SNR of the received signal at the ED is given as

$$\gamma_e = \frac{\alpha p \Omega^2 d_{ub}^{-2} d_{be}^{-2}}{q \Omega d_{ue}^{-2} + \alpha q \Omega^2 d_{ub}^{-2} d_{be}^{-2} + \sigma_e^2} \tag{7}$$

The secrecy rate of the BD transmission is given as [5], [9]

$$R_{sec} = [\log_2(1 + \gamma_u) - \log_2(1 + \gamma_e)]^+ \tag{8}$$

III. Joint Power and Location Optimization

In this section, we formulate and solve the optimization problem that maximizes the secrecy rate. Specifically, we optimize the reflection coefficient α, the power allocation factor ϕ, and the hovering position of the UAV x such that the secrecy rate is maximized subject to a predefined constraints. The optimization problem is formulated as follows

$$\mathbf{P1}: \max_{\alpha,\phi,x} R_{sec} \tag{9}$$
$$s.t.\ 0 \le \phi \le 1 \tag{10}$$
$$0 \le \alpha \le 1 \tag{11}$$

Considering the worst case scenario, where the noise at the ED is zero, i.e $\sigma_e^2 = 0$, we analyze and deduce the secrecy rate as follows

$$\begin{aligned} R_{\text{sec}} &= \log_2(1+\gamma_u) - \log_2(1+\gamma_e) \\ &= \log_2(1 + \frac{\alpha\phi P_c\Omega^2}{\kappa\alpha(1-\phi)P_c\Omega^2 + \sigma_u^2 d_{ub}^4}) \\ &- \log_2(1 + \frac{\alpha\phi P_c\Omega^2 d_{ue}^2}{(1-\phi)P_c(\Omega d_{ub}^2 d_{be}^2 + \alpha\Omega^2 d_{ue}^2)}) \\ &= \log_2(1 + \frac{\alpha\phi P_c\Omega^2}{\kappa\alpha(1-\phi)P_c\Omega^2 + \sigma_u^2 d_{ub}^4}) \\ &+ \log_2(\frac{(1-\phi)P_c(\Omega d_{ub}^2 d_{be}^2 + \alpha\Omega^2 d_{ue}^2)}{(1-\phi)P_c\Omega d_{ub}^2 d_{be}^2 + \alpha P_c\Omega^2 d_{ue}^2}) \\ &= \log_2(1 + \frac{f_1(\alpha,\phi,x)}{g_1(\alpha,\phi,x)}) + \log_2(\frac{f_2(\alpha,\phi,x)}{g_2(\alpha,\phi,x)}) \end{aligned} \tag{12}$$

Since the problem is a non-convex problem, we consider designing an iterative algorithm based on the AO algorithm to solve it.

A. Reflection coefficient optimization

Considering fixed power allocation factor and hover point of the UAV, the following problem (P2) optimises the reflection coefficient of BD as follows

$$\mathbf{P2}: \max_{\alpha} R_{sec} \tag{13}$$
$$0 \le \alpha \le 1 \tag{14}$$

We can reformulate the secrecy rate as follows

$$R_{\text{sec}} = \log_2(1 + \frac{f_1(\alpha)}{g_1(\alpha)}) + \log_2(\frac{f_2(\alpha)}{g_2(\alpha)}) \tag{15}$$

Note that the functions $f_1(\alpha), f_2(\alpha), g_1(\alpha), g_2(\alpha)$ are linear functions of variable α, meeting the characteristics that the numerator is concave function and the denominator is convex function, and $f_1(\alpha) >= 0, f_2(\alpha) >= 0, g_1(\alpha) > 0, g_2(\alpha) > 0$ and $\log_2(\cdot)$ function is concave and monotonically increasing. So, problem (P2) is a multiple concave-convex fractional programming (FP) optimization problem and it can be transformed by quadratic transform according to corollary 2 in [17]. Thus, the problem (P2) can be converted into problem (P3) as follows

$$\begin{aligned} \mathbf{P3}: \max_{\alpha}\ & R_{sec} = \log_2(1 + 2y_1\sqrt{f_1(\alpha)} - {y_1}^2 g_1(\alpha)) \\ & + \log_2(2y_2\sqrt{f_2(\alpha)} - {y_2}^2 g_2(\alpha)) \end{aligned} \tag{16}$$
$$0 \le \alpha \le 1 \tag{17}$$

where y_1, y_2 are the auxiliary variables, and the optimal y_1, y_2 can be obtained by iterative method as follows

$$y_m^{(i)} = \frac{\sqrt{f_m^{(i-1)}(\alpha)}}{g_m^{(i-1)}(\alpha)}, m = 1, 2 \tag{18}$$

where i is the number of iterations. When y_m is fixed, as each $f_m(\alpha)$ is concave, each $g_m(\alpha)$ is convex and the square-root function is concave and increasing, the quadratic transform

$$\chi(\alpha, y_m) = 2y_m\sqrt{f_m(\alpha)} - y_m^2 g_m(\alpha),\ m = 1, 2 \tag{19}$$

is concave in α for fixed y_m. Further, because $\log(\cdot)$ is concave and monotonically increasing, then it can be concluded that $\log(\chi(\alpha, y_m))$ is concave in α. Therefore, the problem (P3) is concave maximization problem over α and common convex optimization methods, such as the interior point method, can be utilized to solve this problem.

B. Power allocation factor optimization

Considering fixed hovering point of the UAV and the reflection coefficient of the BD, the following problem (P4) optimises the power allocation factor

$$\mathbf{P4}: \max_{\phi} R_{sec} \tag{20}$$
$$0 \le \phi \le 1 \tag{21}$$

We can reformulate the secrecy rate as follows

$$R_{\text{sec}} = \log_2(1 + \frac{f_1(\phi)}{g_1(\phi)}) + \log_2(\frac{f_2(\phi)}{g_2(\phi)}) \tag{22}$$

Similarly, problem (P4) is a concave-convex FP optimization problem and can be converted into question (P5) as follows

$$\begin{aligned} \mathbf{P5}: \max_{\phi}\ & R_{sec} = \log_2(1 + 2y_1\sqrt{f_1(\phi)} - {y_1}^2 g_1(\phi)) \\ & + \log_2(2y_2\sqrt{f_2(\phi)} - {y_2}^2 g_2(\phi)) \end{aligned} \tag{23}$$
$$0 \le \phi \le 1 \tag{24}$$

Likewise, it is easy to conclude that the quadratic transformed problems (P5) is concave maximization problem over ϕ and can be solved by common convex optimization methods.

C. Flight position optimization

Considering fixed reflection coefficient and power allocation factor, the following problem (P6) optimises the hovering point of the UAV

$$\mathbf{P6}: \max_{x} R_{sec} \tag{25}$$

We consider introducing relaxation variables v, w to meet the following requirements

$$d_{ub}^2 = (x - x_b)^2 + H^2 \le v \tag{26}$$
$$d_{ue}^2 = (x - x_e)^2 + H^2 \le w \tag{27}$$

We can reformulate the secrecy rate as follows

$$\begin{aligned} R_{\text{sec}} &= \log_2(1+\frac{f_1(v,w)}{g_1(v,w)})+\log_2(\frac{f_2(v,w)}{g_2(v,w)}) \\ &=\log_2(1+\frac{\alpha\phi P_c\Omega^2}{\kappa\alpha(1-\phi)P_c\Omega^2+\sigma_u^2 v^2}) \\ &+\log_2(\frac{(1-\phi)P_c(\Omega d_{be}^2 v+\alpha\Omega^2 w)}{(1-\phi)P_c\Omega d_{be}^2 v+\alpha P_c\Omega^2 w}) \end{aligned} \tag{28}$$

Similarly, problem (P6) is a concave-convex FP optimization problem and can be converted into question (P7) as follows

$$\begin{aligned} \mathbf{P7}: \max_{x,v,w}\ & R_{sec}=\log_2(1+2y_1\sqrt{f_1(v,w)}-{y_1}^2 g_1(v,w)) \\ &+\log_2(2y_2\sqrt{f_2(v,w)}-{y_2}^2 g_2(v,w)) && (29) \\ & (x-x_b)^2+H^2\le v && (30) \\ & (x-x_e)^2+H^2\le w && (31) \end{aligned}$$

Likewise, it is easy to conclude that the quadratic transformed problems (P7) is concave maximization problem over v, w and can be solved by convex optimization methods.

D. Joint iterative algorithm

In order to solve (P1), this paper designs an iterative algorithm based on the alternating optimization (AO) algorithm. The pseudo code is provided in Algorithm 1. The optimization results of the reflection coefficient of BD, power allocation factor of UAV, and the optimal hover point of UAV are alternately updated to obtain the sub-optimal solution. By iteratively solving (P3), (P5), and (P7), we can obtain the approximate local optimal value of (P1). And because R_{sec} is a finite value and the optimal solution obtained by each iteration is not reduced, the iterative algorithm is guaranteed to converge.

IV. Numerical Results

In this section, we assess the performance of the proposed system through numerical evaluation. Unless otherwise stated, we set $x_b = 7\text{m}$, $x_e = 8\text{m}$, $\kappa = 0.1$, the transmit frequency $f = 755\text{MHz}$, $P_c = 30\text{dBm}$, $\varpi = 2$, and $\sigma_u^2 = -60\text{dbm}$.

Fig. 2 describes the convergence curves of the designed algorithms. Fig. 2a depicts the convergence of solving each subproblem by using the quadratic transform method and iteratively updating the y_1 and y_2 parameters where the flying altitude of UAV is 3m. The simulation results show that our quadratic transform method has a fast convergence rate. Fig. 2b depicts the convergence of the whole AO algorithm. The simulation results demonstrate that our AO algorithm exhibits a rapid convergence rate.

Fig. 3 illustrates the relationship between the maximum secrecy rate and the noise attenuation factor κ at different heights of the UAV. The simulation results reveal a gradual reduction in the secrecy rate as the noise attenuation factor increases. When the height of the UAV is in close proximity, the decline becomes more pronounced. However, when the height of the UAV is high, the noise attenuation factor has little impact on the secrecy rate.

Algorithm 1 The algorithm for solving (P1)

Require: transmit power of UAV, vertical altitude of UAV flight, location of backscatter equipment and eavesdropper, noise power, convergence threshold ϵ,

Ensure: Optimal ϕ, α, x, and maximum R_{sec}.

1: Initialise feasible $\phi^{(0)}$, $\alpha^{(0)}$, $x^{(0)}$;
2: Initialise $R_{sec}^{(0)}$ by substituting $\phi^{(0)}$, $\alpha^{(0)}$, $x^{(0)}$ into (12);
3: Initialise $R_{sec}^{(-1)} \leftarrow 0$ and $i \leftarrow 0$;
4: **while** $|R_{sec}^{(i)} - R_{sec}^{(i-1)}| > \epsilon$ **do**
5: Update $i \leftarrow i+1$;
6: Obtain optimal α^i, by iteratively updating y_1,y_2 first by the formula (18), and then solving (P3) with $\phi^{(i-1)}$, $x^{(i-1)}$ and the updated y_1,y_2 of each iteration until convergence;
7: Obtain optimal ϕ^i, by iteratively updating y_1,y_2 first by the formula (18), and then solving (P5) with $\alpha^{(i)}$, $x^{(i-1)}$ and the updated y_1,y_2 of each iteration until convergence;
8: Obtain optimal $x^{(i)}$, by iteratively updating y_1,y_2 first by the formula (18), and then solving (P7) with $\phi^{(i)}$, $\alpha^{(i)}$ and the updated y_1,y_2 of each iteration until convergence;
9: **end while**
10: **return** $\phi^{(*)}$, $\alpha^{(*)}$, $x^{(*)}$, $R_{sec}^{(*)}$.

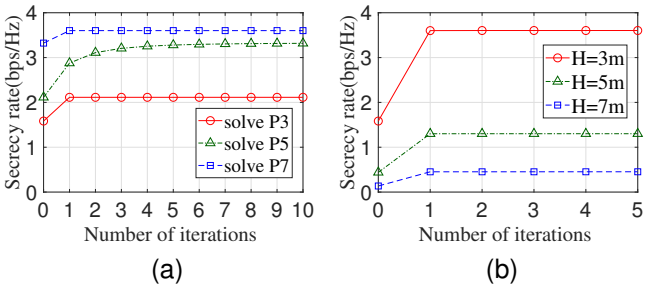

Fig. 2. Convergence analysis: (a) convergence diagram of each subproblem, (b) convergence diagram of the whole algorithm.

Fig. 4 depicts the relationship between the optimal power allocation factor ϕ and the distance between the ED and the BD d_{be} under different flight altitudes. The simulation results indicate that only a small fraction of the total power is required as AN to maximize the secrecy rate. Additionally, as the distance between the ED and the BD increases, a lower fraction of power is needed for AN in order to achieve optimal secrecy performance. It can also be seen that the higher the altitude of UAV, the lower the power allocation factor. This also implies (although not shown in the figure) that the lower the transmit power budget at the UAV, the higher fraction of the total power is required for noise injection.

Fig. 5 depicts the relationship between the secrecy rate and power allocation factor ϕ under different values of the reflection coefficient α. It can be seen that the secrecy rate first increases and then decreases with ϕ, and there exists a maximum value. It is worth noting that the small circles on the curves represent the optimal power allocation factor, which

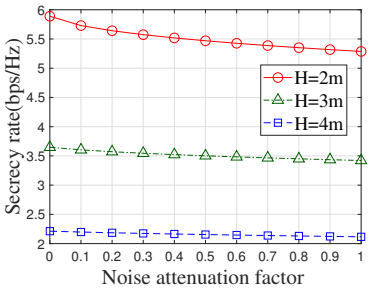

Fig. 3. Secrecy rate versus the noise attenuation factor κ at different heights of the UAV.

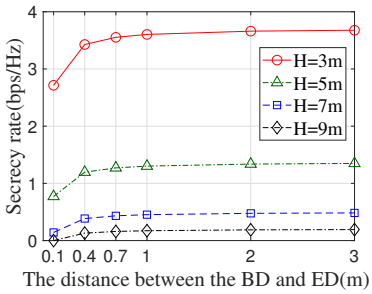

Fig. 6. The relationship between the secrecy rate and the distance between the BD and ED d_{be}.

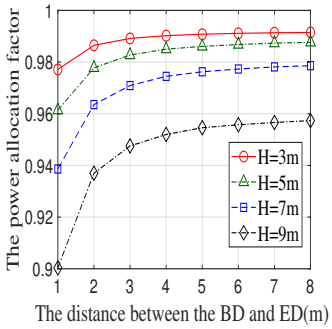

Fig. 4. The relationship between the power allocation factor ϕ and the distance between the BD and the ED, d_{be}.

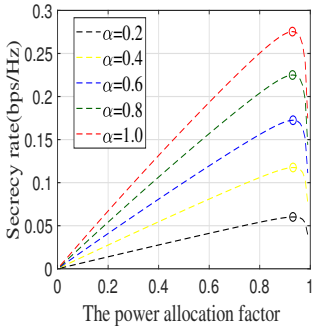

Fig. 5. Secrecy rate versus power allocation factor ϕ with different values of the reflection coefficient α.

verifies the effectiveness of our algorithm. Besides, it can be seen that as the reflection coefficient increases, the secrecy rate increases.

Fig. 6 shows the effect of varying the distance between the BD and the ED on the secrecy performance for various flight altitudes. The figure reveals that the secrecy rate strongly depends on the BD-ED distance when this distance is small, i. e., in the range from 0.1 meters to 1 meter. However, the figure shows the effectiveness of our AN scheme, where we still has good secrecy rate performance even when the distance between the BD and the ED is relatively small. In addition, it can be seen that the UAV altitude has strong effect on the secrecy performance. For instance, when the BD-ED distance is 0.2 meters, about 3 bps/Hz is achieved when H=3m compared with 1 bps/Hz when when H=5m.

V. Conclusions

In this paper, we addressed the problem of physical layer security in UAV-assisted backscatter communications. We proposed AN-assisted transmission scheme to improve the secure transmission of the proposed system. We designed an optimization algorithm to maximize the secrecy rate, wherein we conducted joint optimization of the UAV's hovering position, the power allocation of the UAV, and the reflection coefficient at the BD. It was shown that the AN can significantly improve the secrecy performance of the proposed UAV-assisted backscatter system. The effect of the different system parameters such as the hovering height and noise cancellation factor on the secrecy performance were also investigated.

References

[1] C. Xu, L. Yang, and P. Zhang, "Practical backscatter communication systems for battery-free Internet of things: A tutorial and survey of recent research," *IEEE Signal Process. Mag.*, vol. 35, no. 5, pp. 16–27, Sep. 2018.

[2] C. Zhan, Y. Zeng, and R. Zhang, "Energy-efficient data collection in UAV enabled wireless sensor network," *IEEE Wireless Commun. Lett.*, vol. 7, no. 3, pp. 328–331, 2018.

[3] S. Yang, Y. Deng, X. Tang, Y. Ding, and J. Zhou, "Energy efficiency optimization for UAV-assisted backscatter communications," *IEEE Commun. Lett.*, vol. 23, no. 11, pp. 2041–2045, 2019.

[4] R. Han, L. Bai, Y. Wen, J. Liu, J. Choi, and W. Zhang, "UAV-aided backscatter communications: Performance analysis and trajectory optimization," *IEEE J. Sel. Areas Commun.*, vol. 39, no. 10, pp. 3129–3143, 2021.

[5] W. Saad, X. Zhou, Z. Han, and H. V. Poor, "On the physical layer security of backscatter wireless systems," *IEEE Trans. Wireless Commun.*, vol. 13, no. 6, pp. 3442–3451, 2014.

[6] Y. Zhang, F. Gao, L. Fan, X. Lei, and G. K. Karagiannidis, "Secure communications for multi-tag backscatter systems," *IEEE Wireless Commun. Lett.*, vol. 8, no. 4, pp. 1146–1149, 2019.

[7] Q. Yang, H.-M. Wang, Y. Zhang, and Z. Han, "Physical layer security in MIMO backscatter wireless systems," *IEEE Trans. on Wireless Commun.*, vol. 15, no. 11, pp. 7547–7560, 2016.

[8] P. Wang, Z. Yan, N. Wang, and K. Zeng, "Resource allocation optimization for secure multidevice wirelessly powered backscatter communication with artificial noise," *IEEE Transactions on Wireless Communications*, vol. 21, no. 9, pp. 7794–7809, 2022.

[9] A. Al-Nahar, R. Jäntti, G. Zheng, D. Mishra, and M. Nie, "Ergodic secrecy rate analysis and optimal power allocation for symbiotic radio networks," *IEEE Access*, vol. 11, pp. 82 327–82 337, 2023.

[10] X. Zhou, S. Yan, J. Hu, J. Sun, J. Li, and F. Shu, "Joint optimization of a UAV's trajectory and transmit power for covert communications," *IEEE Trans. on Signal Process.*, vol. 67, no. 16, pp. 4276–4290, 2019.

[11] J. Hu, X. Cai, and K. Yang, "Joint trajectory and scheduling design for UAV aided secure backscatter communications," *IEEE Wireless Commun. Lett.*, vol. 9, no. 12, pp. 2168–2172, 2020.

[12] L. Bai, Q. Chen, T. Bai, and J. Wang, "UAV-enabled secure multiuser backscatter communications with planar array," *IEEE J. Sel. Areas Commun.*, vol. 40, no. 10, pp. 2946–2961, 2022.

[13] S. Goel and R. Negi, "Guaranteeing secrecy using artificial noise," *IEEE Trans. Wireless Commun.*, vol. 7, no. 6, pp. 2180–2189, 2008.

[14] A. Al-Nahari, G. Geraci, M. Al-Jamali, M. H. Ahmed, and N. Yang, "Beamforming with artificial noise for secure MISOME cognitive radio transmissions," *IEEE Trans. Inf. Forensics Secur.*, vol. 13, no. 8, pp. 1875–1889, 2018.

[15] N. V. Huynh, D. T. Hoang, X. Lu, D. Niyato, P. Wang, and D. I. Kim, "Ambient backscatter communications: A contemporary survey," *IEEE Commun. Surveys Tuts.*, vol. 20, no. 4, pp. 2889–2922, 4th Quart. 2018.

[16] R. Long, Y.-C. Liang, H. Guo, G. Yang, and R. Zhang, "Symbiotic radio: A new communication paradigm for passive Internet of Things," *IEEE Internet Things J.*, vol. 7, no. 2, pp. 1350–1363, 2020.

[17] K. Shen and W. Yu, "Fractional programming for communication systems—part i: Power control and beamforming," *IEEE Trans. Signal Process.*, vol. 66, no. 10, pp. 2616–2630, 2018.